

Anti-parity-time topologically undefined state

HAOHAO WANG¹, KAIWEN JI^{1,5}, YUANDAN WANG¹, ZHENJUAN LIU¹, YUANMEI GAO², YANLONG SHEN³, SHI BAI⁴, KOJI SUGIOKA⁴, AND XINYUAN QI^{1*}

¹School of Physics, Northwest University, 710127, Xi'an, China

²College of Physics and Electronics, Shandong Normal University, Jinan, 250014, China

³State Key Laboratory of Laser Interaction with Matter, Northwest Institute of Nuclear Technology, Xi'an Shaanxi 710024, China

⁴RIKEN Center for Advanced Photonics, Hirosawa 2-1, Wako, Saitama 351-0198, Japan

⁵Centre for Nanosciences and Nanotechnologies, Université Paris-Saclay, Palaiseau, France

*Corresponding author: qixycn@nwnu.edu.cn

Compiled January 6, 2022

We constructed an anti-parity-time-symmetric photonic lattice by using perturbations. The results show the topological state will appear when the waveguide coupling constants $\kappa_1 < \kappa_2$; Interestingly, a state with undefined winding numbers occurs when $\kappa_1 = \kappa_2$, in which the light distributes only in the wide waveguides with equal magnitude distribution. Further studies show that the edge state will be strengthened by introducing defect for the topologically non-trivial case, while it will not affect the equal intensity transmission for the topologically undefined state. Our work provides a new way to realize the topological state and equally divided light transmission and might be applicable in optical circuits and optical interconnect. © 2022 Optical Society of America

<http://dx.doi.org/10.1364/ao.XX.XXXXXX>

1. INTRODUCTION

Topological photonics, as one of the most remarkable topics, is inspired from the discovery of the quantum Hall effects and the topological insulators in the condensed matter [1, 2]. In recent years, a variety of discrete photonic systems have been proved to realize the topological phase [3], such as the Floquet topological insulators with spatial modulation based on the array of laser-written optical waveguides [4] and a network of surface plasmon rings [5], topological photonics in meta-waveguides [6] and photonic topological insulators [7]. Based on these studies, a large number of phenomena have emerged, such as the topologically protected edge states and corner states in photonic crystals [8], slow light [9], nonlinear optical isolation [10]. Clearly, a common feature of these studies is that the systems must be Hermitian, which means the topological invariant of a system with open boundary condition could be judged by the bulk-edge correspondence [11].

In the non-Hermitian systems where there exists energy exchange with the ambient environment, the fractional winding number could be observed, and the usual bulk-edge correspondence is invalid [12]. The global Berry phase [13], the non-

Bloch winding number [14, 15], and the Kronecker index [16] could be employed to calculate the winding numbers. These findings promote the development of topology research in the non-Hermitian system [3, 17–21]. The propagation of light in these systems will be affected by external conditions, leading to many novel phenomena, such as lasing generation in topological edge states of a polariton micropillar array [3], fermi nodal disk in magnetic plasma [17], skin effects [18, 19], boundary modes [19], exceptional non-Hermitian topological edge mode [20], and anomalous topological edge state [21] and so on.

However, there exists a particular state with an undefined topological invariant in all of these studies. For the two-band model, once the closed parametric curve of the coefficient vector $d(k)$ of bulk momentum-space Hamiltonian $\hat{H}(k)$ is tangent to the origin, the winding number is undefined [22], which means that such a topologically undefined state is a critical state between the topologically non-trivial and topologically trivial ones. Considering the signs around the Dirac point in two-dimensional systems are opposite while the dispersion surface around the Weyl points is changed dramatically [3, 23], most of the current studies are focused on the linear regions, and therefore the studies of light dynamics at these points are still remarkably absent.

In this Letter, we propose a one-dimensional anti-parity-time-symmetric (anti-PT) photonic lattice with perturbations. By eliminating the amplitudes of the perturbation sites adiabatically, we obtained an effective Hamiltonian with anti-PT symmetry. The system is proved theoretically to be topologically non-trivial when the coupling constants $\kappa_1 < \kappa_2$; while there exists a topologically undefined state when $\kappa_1 = \kappa_2$. It is also found that the introduction of the defect will strengthen the edge state for the topologically non-trivial case while it will not affect the equal intensity transmission for the topologically undefined state. Our study enriches the physics of topological photonics and paves a new way to achieve the topological edge state and undefined state, which might have potential applications in the fields of optical circuits and optical communication.

2. MODEL AND ANALYSIS

We construct a one-dimensional photonic lattice with perturbations, as shown in Fig. 1(a). ρ_n , a_n , and b_n are the light

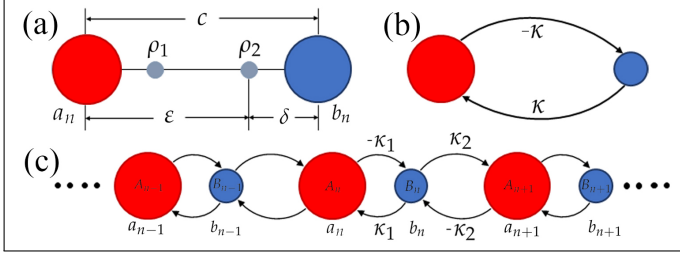


Fig. 1. Schematic of photonic lattices with perturbations. (a) Perturbations used to realize anti-PT symmetry. (b) Effective model. (c) Periodic anti-PT structure. ρ_n , the perturbation sites (the gray sites); A_n (the red sites) and B_n (the blue sites) are wide and narrow waveguides, respectively. $\kappa_{1,2} > 0$ are the coupling constants.

amplitudes of the perturbation site, ordinary waveguides A_n and B_n , respectively. Assuming that the refractive index of the perturbation site is much smaller than those on sites A_n and B_n , $n_p \ll n_{a,b}$, therefore the modal amplitudes in the ordinary waveguides are more substantial than in the perturbations [24]. Accordingly, the ordinary waveguide will not be affected by the next neighbor perturbation. Under the above conditions, the Hamiltonian of the periodic system, H' , with perturbations is described as

$$H' = \begin{pmatrix} \beta_a & c & \delta & 0 \\ c & \beta_b & 0 & \delta \\ \delta & \epsilon & \beta_{\rho,1} & 0 \\ \epsilon & \delta & 0 & \beta_{\rho,2} \end{pmatrix}, \quad (1)$$

where δ and ϵ are the nearest and next-nearest coupling constants between the perturbations and the ordinary waveguides. c is the coupling constant between ordinary waveguides. β is the propagation constant. One can describe the evolution of this system by the Schrödinger-like equation [25] $i \frac{d\psi'_n}{dz} = H' \psi'_n$ and the wave functions of $\psi'_n = [a_n, b_n, \rho_1, \rho_2]^T$.

To simplify the equations, one can eliminate the amplitudes of perturbation sites ρ_n adiabatically [26],

$$\rho_1 \approx \frac{-a\delta - b\epsilon}{\beta_{\rho,1}}, \rho_2 \approx \frac{-b\delta - a\epsilon}{\beta_{\rho,2}}. \quad (2)$$

After setting the propagation constants of the perturbation sites as $\beta_{\rho,1} = \delta\epsilon/(c - \kappa)$, $\beta_{\rho,2} = \delta\epsilon/(c + \kappa)$ and those for the ordinary waveguides as $\beta_a = (c\delta + \Delta\epsilon - \delta\kappa)/\epsilon$ and $\beta_b = (c\delta - \Delta\epsilon + \delta\kappa)/\epsilon$, one can obtain the effective Hamiltonian

$$H = \begin{pmatrix} \Delta & \kappa \\ -\kappa & -\Delta \end{pmatrix}, \quad (3)$$

where Δ and κ are the corresponding effective propagation constant and coupling constant, respectively. The simplified system is shown in Fig. 1(b). The effective Hamiltonian satisfies $PTH + HPT = 0$, where $P = \sigma_x$ and $T = IK$ are the parity and time operators, respectively. $\sigma_{x,y,z}$ are the Pauli matrices, I is the identity operator, K is the elementwise complex conjugation in the effective Hamiltonian. Apparently, the effective Hamiltonian of such a system satisfies anti-PT symmetry but is not chirally symmetric, $\Gamma H \Gamma^{-1} \neq -H$, where $\Gamma = \sigma_z$.

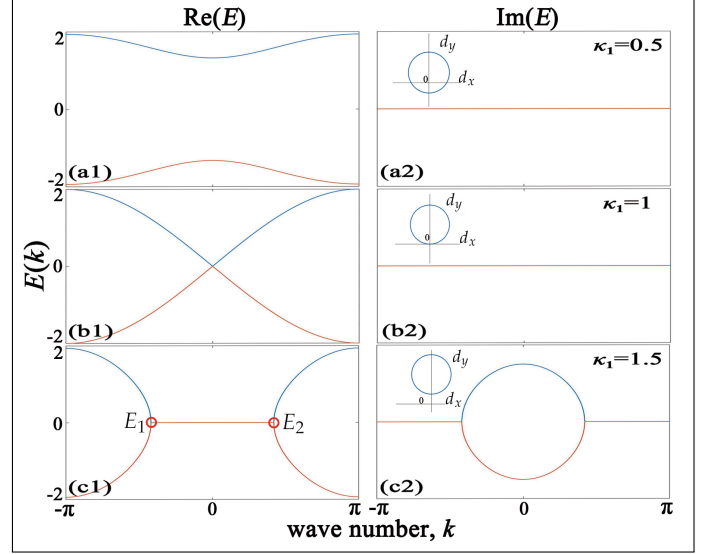


Fig. 2. Bulk band structure with different κ_1 .

As shown in the aforementioned analysis, we have realized an anti-PT symmetric optical coupler. Based on this, we employ such a configuration to construct a topological Su-Schrieffer-Heeger (SSH) model [3] [see Fig. 1(c)]. The Bloch Hamiltonian of such a periodic system is

$$H = -id_x\sigma_x + id_y\sigma_y + \Delta\sigma_z, \quad (4)$$

$$d_x = \kappa_2 \sin k, \quad (5)$$

$$d_y = \kappa_1 + \kappa_2 \cos k, \quad (6)$$

where κ_1 and κ_2 are the coupling constants inside and outside one cell. One can learn that the Hamiltonian satisfies $\{H, \tau\} = 0$, where $\tau = \sigma_x K$, in other words, the system has non-Hermitian particle-hole symmetry, which guarantees that the eigenvalues always appear in pair $\pm E(k)$. The corresponding eigenvalues of the bulk Hamiltonian read

$$E(k) = \pm \sqrt{\Delta^2 - d_x^2 - d_y^2}. \quad (7)$$

The eigenvalues of the bulk Hamiltonian are demonstrated in Fig. 2, one can notice that the two bands are closing to each other with the increasing κ_1 , and a Dirac point is formed at $k = 0$ when $\kappa_1 = 1$ [see Fig. 2(b1)]. It is also shown in the inset in Fig. 2(b2) that the circle is tangent to the origin in the inset, this indicates that the winding number of the system is undefined. Further increasing the magnitude of the inner coupling constant κ_1 , a flatband starts to emerge in the center of the Brillouin zone as a result of the protection of non-Hermitian particle-hole symmetry [see Fig. 2(c1)]. Such a flatband covers a region of $-\sqrt{d_x^2 + d_y^2} < \Delta < \sqrt{d_x^2 + d_y^2}$ in which E_1 and E_2 are also known as the exceptional points [27]. We further calculated the winding number W of such a system [25]. It is shown $W = 1$ corresponding to a topological non-trivial state when $\kappa_1 < \kappa_2$, and $W = \frac{1}{2}$ corresponding to an undefined state when $\kappa_1 = \kappa_2$.

The open boundary spectra are given in Fig. 3. Two non-zero edge modes occur when $\kappa_2 - \Delta < \kappa_1 < \Delta - \kappa_2$ in Fig. 3(a) and (b), suggesting the ordinary bulk-boundary correspondence is valid in our non-Hermitian anti-PT symmetric system. As shown in Fig. 3(c), two new non-zero defect modes form (the

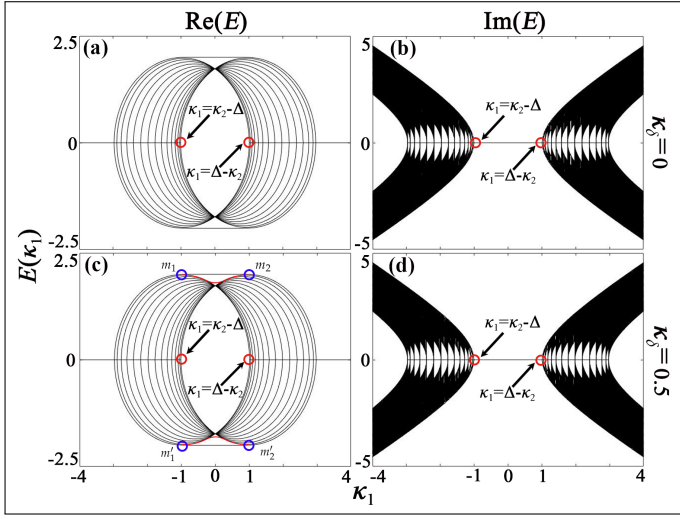


Fig. 3. Band structure as a function of κ_1 in the SSH model with open boundary. Here, the total number of the waveguide is $N = 30$, $\kappa_2 = 1$, $\kappa_\delta = 0.5$, $\Delta = 2$. (a) and (b) are the real and imaginary parts of eigenvalues. (c) and (d) are spectra with a defect at the left-most site.

red lines between m_1 and m_2 , m'_1 and m'_2) when a defect is introduced in the left-most edge by replacing the coupling constant κ_1 with $\kappa_1 + \kappa_\delta$ to test the robustness of the system. Clearly, the defect modes do not break the topological edge modes and the region of κ_1 is also unchanged [Fig. 3(d)], proving that the edge modes are robust to the defect due to topological protection.

To further investigate the energy distribution for the topological state, the stationary Schrödinger-like equation

$$(E - \Delta)a_n = \kappa_1 b_n + \kappa_2 b_{n-1}, \quad (8)$$

$$(E + \Delta)b_n = -\kappa_1 a_n - \kappa_2 a_{n+1}. \quad (9)$$

is used. As the band analysis predicts that the left edge mode has an eigenvalue of $E_{left} = \Delta$, with the boundary conditions

$$(E - \Delta)a_0 = \kappa_1 b_0, \quad (10)$$

$$(E + \Delta)b_0 = -\kappa_1 a_0 - \kappa_2 a_1. \quad (11)$$

One can learn that

$$b_n = 0, \quad (12)$$

$$|a_n|^2 = \left(\frac{\kappa_1}{\kappa_2}\right)^{2n} |a_0|^2. \quad (13)$$

This indicates that the left incidence a_0 can induce a particular energy distribution a_n and the energy only exists at the wide waveguide, site A_n . Peculiarly, a stable edge mode forms when $\kappa_1 < \kappa_2$, which agrees with the topological edge state. When $\kappa_1 = \kappa_2$, it is seen from Eq. 13 $|a_n|^2 = |a_0|^2$, indicating that the light energy distributes equally in all the wide waveguides A_n for the case with undefined winding number [see Fig. 2(b2)]. Figuratively speaking, the topological state has been "copied" to all the waveguides A_n for this special state.

Further considering the defect $\kappa_\delta \geq 0$ in the first cell, one can get the following relations,

$$(E - \Delta)a_0 = (\kappa_1 + \kappa_\delta)b_0, \quad (14)$$

$$(E + \Delta)b_0 = -(\kappa_1 - \kappa_\delta)a_0 - \kappa_2 a_1, \quad (15)$$

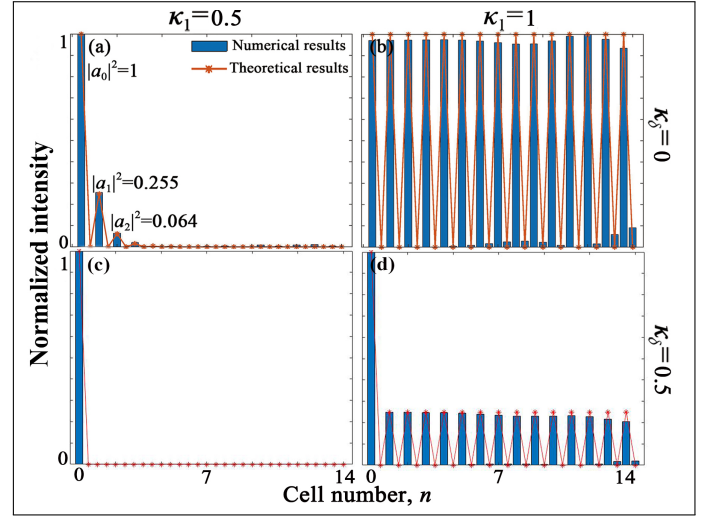


Fig. 4. Numerical calculations of output energy distribution in both (a) topologically non-trivial ($\kappa_1 = 0.5$) and (b) undefined cases ($\kappa_1 = 1$). (c) and (d) add the defect at the edge with different κ_1 and same κ_δ .

and obtain similar results with defect κ_δ ,

$$b_n = 0, \quad (16)$$

$$|a_n|^2 = \left(\frac{\kappa_1}{\kappa_2}\right)^{2n} \left(\frac{\kappa_1 - \kappa_\delta}{\kappa_1}\right)^2 |a_0|^2. \quad (17)$$

Considering the modulated coupling constants should not break the lattice symmetry [see Fig. 1(c)], the coefficient term of a_0 on the right-hand side in Eq. 15 should satisfy $\kappa_1 - \kappa_\delta \geq 0$. Therefore the defect $0 \leq \kappa_\delta \leq \kappa_1$ is deduced. Since the imaginary part of the energy spectrum is zero for both the topological state [Fig. 2(a1) and (a2)] and undefined state [Fig. 2(b1) and (b2)], it is easy to find from Eq. 17 that $|a_n|^2 \leq |a_0|^2$, indicating that the strongest light energy still distributes in the first waveguide A_0 and the light field in other waveguides A_n can be controlled by adjusting the coupling constants κ_1 , κ_2 and defect κ_δ .

To see the characteristics of the system more vividly, we calculated the output energy distribution both numerically and theoretically. As shown in Fig. 4, the energy will only reside on the sites A_n when the left edge mode is excited for $\kappa_1 < \kappa_2$ [see Fig. 4(a)]. The edge state will be strengthened when the defect is introduced ($\kappa_\delta = 0.5$), namely, the system is topologically nontrivial [see Fig. 4(c)]. Interesting, it is found that all the light intensity has the same magnitudes when $\kappa_1 = \kappa_2$ and $\kappa_\delta = 0$, for which the winding number of the system is undefined [see the inset in Fig. 2(b2)]. When $\kappa_1 = \kappa_2$ and $\kappa_\delta = 0.5$, the equal intensity distribution keeps except for the first waveguide A_0 , this means that this kind of undefined state is also robust and be immune to the defect [Fig. 4(d)].

Figure 5 shows the numerical simulation of light propagation in our system. Most of the light energy will be localized on waveguide A_0 and propagates along with it for an incident beam with a function of $e^{-\left(\frac{n-n_0}{\omega_0}\right)^2}$ ($\omega_0 = 0.1$) when $\kappa_1 < \kappa_2$ [see Fig. 5(a)]. When $\kappa_1 = \kappa_2 = 1$, the light will be coupled to the next nearest waveguides and finally propagates in all the sites A_n ($n \in [0, 14]$) with equal intensities [see Fig. 5(b)]. Contrastly, light wave is localized completely at A_0 when the defect is introduced ($\kappa_\delta = 0.5$) [see Fig. 5(c)]; This kind of strong

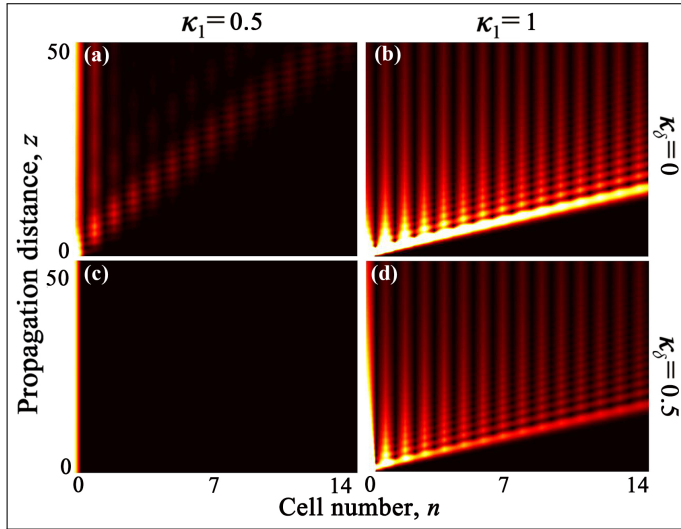


Fig. 5. Numerical simulation of light propagation incident from the left-most waveguide A_0 .

localization could be attributed to the co-action of topological edge state and the defect mode as shown in Fig. 3(c) and Fig. 4(c). For the case of $\kappa_1 = 1$ and $\kappa_\delta = 0.5$ [Fig. 5(d)], the light will also distribute evenly in all the A_n waveguides except that the first waveguide has larger energy due to the defect. Apparently, the light propagation is in good agreement with the former theoretical and numerical results.

An applicable experimental proposal could be performed with the setup shown in Ref. [27, 28]. A femtosecond laser pulse @1064 nm is focused through a micro-objective lens with 20 times magnification. The wide(site A_n) and narrow(site B_n) waveguides could be induced in the fused silica glass by moving the optical platform relatively. The width and coupling coefficient of the waveguide can be modulated by controlling the moving velocity and the power of the femtosecond laser. A 632.8 nm He-Ne laser can be used as the excitation light source to probe the light dynamics.

In summary, we present an anti-PT symmetric topological photonic lattice with perturbations. The topological edge state and undefined state can both be achieved in such an anti-PT photonic system by tuning the coupling constant. When the coupling constant $\kappa_1 < \kappa_2$, most light transmits at the edge site A_0 , forming a topological state. It is also found that the light distributes equally on all the wide waveguides A_n when $\kappa_1 = \kappa_2$, corresponding to a winding number undefined state. Further study shows the topological edge state will be immune to the defect and might be helpful to the formation of a more localized edge state, while the topologically undefined state is also robust to the defect except for the first waveguide where the input light is incident. Our work enriches the study of topologically undefined states and may offer important applications in optical circuits and optical communications in the future.

3. FUNDING INFORMATION

This work is supported by the Open fund of Shandong Provincial Key Laboratory of Optics and Photonic Devices(K202008), Open Research Fund of State Key Laboratory of laser Interaction with Matter(SKLLIM1812), and Natural Science Foundation of Shaanxi Province, China(2017JM6014).

4. ACKNOWLEDGE

The author Kaiwen Ji would like to acknowledge the support from China scholarship council (CSC No. 202006970015)

5. DISCLOSURES

The authors declare no conflicts of interest.

REFERENCES

1. M. König, S. Wiedmann, C. Brüne, A. Roth, H. Buhmann, L. W. Molenkamp, X.-L. Qi, and S.-C. Zhang, *Science* **318**, 766 (2007).
2. J. Petráček and V. Kuzmiak, *Phys. Rev. A* **101**, 033805 (2020).
3. T. Ozawa, H. M. Price, A. Amo, N. Goldman, M. Hafezi, L. Lu, M. C. Rechtsman, D. Schuster, J. Simon, O. Zilberberg, and I. Carusotto, *Rev. Mod. Phys.* **91**, 015006 (2019).
4. S. Mukherjee, A. Spracklen, M. Valiente, E. Andersson, P. Öhberg, N. Goldman, and R. R. Thomson, *Nat. Commun.* **8**, 13918 (2017).
5. F. Gao, Z. Gao, X. Shi, Z. Yang, X. Lin, H. Xu, J. D. Joannopoulos, M. Soljačić, H. Chen, L. Lu, Y. Chong, and B. Zhang, *Nat. Commun.* **7**, 11619 (2016).
6. X. Cheng, C. Jouvaud, X. Ni, S. H. Mousavi, A. Z. Genack, and A. B. Khanikaev, *Nat. Mater.* **15**, 542 (2016).
7. L.-H. Wu and X. Hu, *Phys. Rev. Lett.* **114**, 223901 (2015).
8. L. Zhang, Y. Yang, Z.-K. Lin, P. Qin, Q. Chen, F. Gao, E. Li, J.-H. Jiang, B. Zhang, and H. Chen, *Adv. Sci.* **7**, 1902724 (2020).
9. L. Yu, H. Xue, and B. Zhang, *Appl. Phys. Lett.* **118**, 071102 (2021).
10. X. Zhou, Y. Wang, D. Leykam, and Y. D. Chong, *New J. Phys.* **19**, 095002 (2017).
11. Y. Hatsugai, *Phys. Rev. Lett.* **71**, 3697 (1993).
12. T. E. Lee, *Phys. Rev. Lett.* **116**, 133903 (2016).
13. S.-D. Liang and G.-Y. Huang, *Phys. Rev. A* **87**, 012118 (2013).
14. S. Yao and Z. Wang, *Phys. Rev. Lett.* **121**, 086803 (2018).
15. L. Jin and Z. Song, *Phys. Rev. B* **99**, 081103 (2019).
16. A. Quandt, *Phys. B: Condens. Matter* **612**, 412867 (2021).
17. W. Wang, W. Gao, L. Cao, Y. Xiang, and S. Zhang, *Light. Sci. & Appl.* **9**, 40 (2020).
18. S. Yao, F. Song, and Z. Wang, *Phys. Rev. Lett.* **121**, 136802 (2018).
19. D. S. Borgnia, A. J. Kruchkov, and R.-J. Slager, *Phys. Rev. Lett.* **124**, 056802 (2020).
20. K. Sone, Y. Ashida, and T. Sagawa, *Nat. Commun.* **11**, 5745 (2020).
21. P. Gao, M. Willatzen, and J. Christensen, *Phys. Rev. Lett.* **125**, 206402 (2020).
22. J. K. Asbóth, L. Oroszlány, and A. Pályi, *A Short Course on Topological Insulators*, vol. 919 of *Lecture Notes in Physics* (Springer International Publishing, Cham).
23. L. Lu, J. D. Joannopoulos, and M. Soljačić, *Nat. Photonics* **8**, 821 (2014).
24. K. Ji, Z. Wen, Z. Liu, Y. Dai, K. Han, P. Gao, A. Gao, J. Bai, G. Zhang, and X. Qi, *Opt. Lett.* **43**, 4457 (2018).
25. K. Ji, Z. Liu, Y. Dai, Z. Wen, Y. Wang, G. Zhang, J. Bai, and X. Qi, *Opt. Lett.* **45**, 49 (2020).
26. S. Longhi, *Phys. Rev. B* **95**, 014201 (2017).
27. S. Xia, D. Kaltsas, D. Song, I. Komis, J. Xu, A. Szameit, H. Buljan, K. G. Makris, and Z. Chen, *Science* **372**, 72 (2021).
28. K. Sugioka and Y. Cheng, *Light. Sci. & Appl.* **3**, e149 (2014).